Optimization of Optical Receiver Parameters for Pulsed Laser Tracking Systems

Zarko P. Barbaric[1], Lazo M. Manojlovic[2]

Abstract – **An analysis of the reception of optical signals on the position sensitive optical receiver is presented in this paper. The optical receiver and electronics for analog signal processing measure the angle displacements between the optical axis of the receiver and the direction optical receiver – designated object, based on current signals, which are generated on the avalanche quadrant photodiode. Special attention was paid to the transimpedance preamplifier and the atmospheric turbulence as the key factors which limit the long range in pulsed laser tracking systems.**

Keywords – **Position sensitive optical receiver, pulsed laser tracking systems, avalanche quadrant photodiode, transimpedance amplifier, atmospheric turbulence.**

I. INTRODUCTION

Today's usage of the pulsed laser systems is very wide in the field of civil and maritime engineering as well as for the military purpose [1]. By using a pulsed laser designator and the corresponding optical receiver some parameters of the laser illuminated object can be determined, such as the distance to the object and its angle displacements. The principle of distance and angle displacements measurements is based on the laser pulses emission, which illuminates the object, whose parameters are to be determined, and their reception with the corresponding optoelectronic receiver [2]. After the analog signal processing, the above mentioned parameters can be determined. By controlling the dynamic range of the received reflected optical radiation and using a well-designed analog signal processing chain, it is possible to reach the accuracy of several millimeters in measuring the distances of several hundreds of meters. To measure the angle displacements it is necessary to use, instead of a standard photodiode, the optical receiver, whose response depends on the light spot position on its surface. There are several types of such an optical receiver, but the quadrant photodiode and the lateral effect photodiode are the most common [3]. The quadrant photodiode is almost exclusively used in pulsed laser tracking systems because of its increased sensitivity and lower

overall noise compared to the lateral effect photodiode. Recently, the avalanche quadrant photodiode with a good matching of each segment avalanche amplification can be found on the market. The advantage in using avalanche quadrant photodiode is in the lower overall noise compared to standard quadrant P-i-N photodiode.

The basic subject of this paper is the optimization of the receiver parameters for pulsed laser tracking systems. The reflected optical radiation from the illuminated object is collected on the receiving optics. The received optical power levels, from the object and the background mostly determine the characteristics of the pulsed laser tracking system. Therefore, the estimations of the received optical powers are given in Part 0. The position sensitive optical detector consists of both the receiving optics and the analog signal processing chain, used for processing signals from the quadrant photodiode. A more detailed description of a position sensitive optical receiver is given in Part 0.

The most significant part of an analog signal processing is the preamplifier. As an optimal solution for the preamplifier the transimpedance amplifier is used. In Part 0 the optimal transimpedance configuration for achieving the minimal overall noise in the receiving chain is presented. The equivalent input noise current was calculated as the optimal avalanche amplification of each avalanche photodiode.

Part 0 shows how the atmospheric turbulence influences the measurement precision. The angle-of-arrival fluctuations and illumination fluctuations were taken into consideration. Finally, in Part 0 the total measurement error was calculated and the optimal receiver parameters for achieving the maximal positioning and tracking range for pulsed laser tracking systems was found.

II. RECEIVED OPTICAL POWERS

For determining the maximum range of the positioning and tracking of objects illuminated by pulsed laser, it is necessary first of all to find the levels of optical powers which we have at the position sensitive optical receiver (PSOR). It is well known that the error of angle measurement is strongly dependent on a signal-to-noise ratio at the output of a receiving chain. In further analysis, the geometrical parameters of the laser designator, illuminated object and of the optical receiver, which are shown on Fig. 1, will serve to find optical power levels at the input of the optical receiver.

[1]Zarko P. Barbaric is with Electrotechnical Faculty, University of Belgrade, Bulevar kralja Aleksandra 73, 11000 Belgrade, Serbia and Montenegro, E-mail: barbaric@etf.bg.ac.yu
[2]Lazo M. Manojlovic is with Pupin Telecom DATACOM, Batajnicki put 23, 11080 Belgrade, Serbia and Montenegro, E-mail: lazom@pupintelecom.co.yu
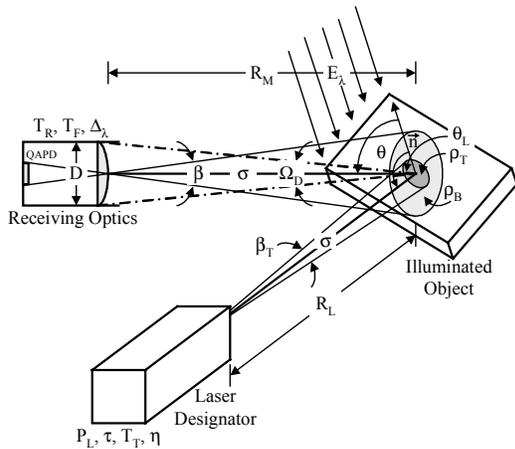
Fig. 1. Geometry of the laser transmitter and the receiving optics.

In the analysis, it is assumed, for the sake of generalization, that the laser designator and the receiving optics are located at different platforms, as it is presented on Fig. 1. Analysis of the optical power levels of a background and reflected laser designator optical signal is conducted on the basics of the well-known radiometrical equation [1]. For the background and the object, it is assumed to be diffuse reflectors which reflecting as a Lambertian source [1]. It is also assumed that the whole laser beam is falling on the surface of the illuminated object.

A. Background Power

The optical power of a background P_B, which is received at the input of an PSOR, is [2]:

$$P_B = L_\lambda G T_R T_F \tau_{at} , \qquad (1)$$

where L_λ is the solar spectral radiance at the object site, G is a geometrical factor, T_R is the receiving optics transmission coefficient, T_F is the optical filter transmission coefficient, τ_{at} is the transmission coefficient of the atmosphere. The geometrical factor G is defined as a factor of radiation exchange of two small areas:

$$G = \frac{A_D \cos\theta \cdot A_R \cos\theta_{po}}{R_M^2} , \qquad (2)$$

where A_D is the area of the detector footprint at the background, $A_R \cos\theta_{po}$ is the effective area of the optical receiver, θ is the angle between object surface normal and the line joining the object and receiver centers, θ_{po} is the angle between the receiver surface normal and the line joining the object and receiver centers ($\theta_{po}=0$, because in the case of good positioning and tracking the receiving optics is always directed towards the object) and R_M is the distance between the object and the optical receiver.
The solar spectral radiance L_λ, induced by solar radiation of a diffuse reflector for a specific wavelength λ is given as [1]:

$$L_\lambda = \frac{E_\lambda \rho_B}{\pi} , \qquad (3)$$

where E_λ is the solar spectral irradiance and ρ_B is the background reflectance.
The atmosphere transmittion coefficient τ_{at} is given as:

$$\tau_{at} = e^{-\sigma R_M} , \qquad (4)$$

where σ is the atmospheric extinction coefficient.
The background power, which is given in Eq. (1), after combining with Eqs. (2) to (4), becomes:

$$P_B = \frac{\pi}{16} E_\lambda \Delta_\lambda \rho_B \beta^2 D^2 T_R T_F e^{-\sigma R_M} , \qquad (5)$$

where Δ_λ is the optical spectral filter bandwidth, β is the receiving optics field-of-view, D is the receiving optics aperture diameter.

B. Signal Power

The received optical signal power P_S, of the reflected laser radiation from the illuminated object, in the case when the area of the laser beam is smaller than the area of the object, is equal to [1-2]:

$$P_S = L_T A_T \Omega_D T_R T_F e^{-\sigma R_M} \cos\theta , \qquad (6)$$

where L_T is the spectral radiance of the reflected radiation from the object, A_T is the area of the laser spot on the object, Ω_D is the solid angle subtended by the optical receiver aperture. The spectral radiance L_T is:

$$L_T = \frac{4 P_L T_T \eta \rho_T e^{-\sigma R_L} \cos\theta_L}{\pi^2 \beta_T^2 R_L^2} , \qquad (7)$$

where P_L is the laser peek power, T_T is the transmission coefficient of transmitting optics, η is the transmitting optics collection efficiency, ρ_T is the target reflectance, θ_L is the angle between the object surface normal and the laser beam, β_T is the laser beam divergence angle and R_L is the distance between the laser and the object.
For the surface A_T of the laser spot on the object the following is valid:

$$A_T = \frac{\pi R_L^2 \beta_T^2}{4 \cos\theta_L} , \qquad (8)$$

and for the solid angle Ω_D:

$$\Omega_D \approx \frac{\pi D^2}{4 R_M^2} . \qquad (9)$$

Combining Eqs. (7) to (9) with Eq. (6), we finally obtain the following for the received signal optical power P_S:

$$P_S = \frac{D^2}{4 R_M^2} P_L \rho_T T_T \eta T_R T_F e^{-\sigma(R_L + R_M)} \cos\theta . \qquad (10)$$

III. THE POSITION SENSITIVE OPTICAL RECEIVER

In this paragraph the principles of the angles of azimuth and elevation measurement using the PSOR and the avalanche quadrant photodiode (AQPD) in pulsed laser tracking systems will be explained. Fig. 2 gives the arrangement of the key optical elements and geometrical parameters of the AQPD in the PSOR.
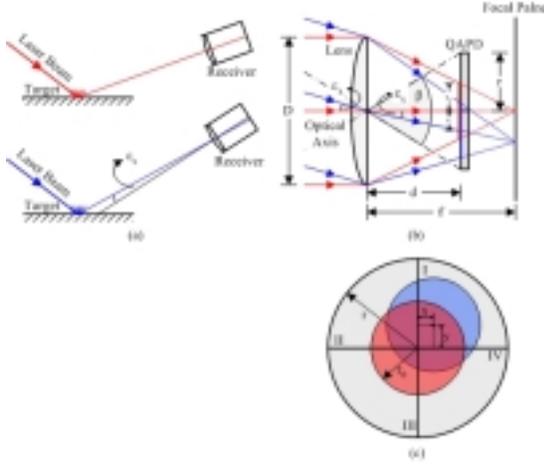

Fig. 2. The PSOR and the AQPD.

The purpose of the optical receiver of the OEC, which is shown on Fig. 2 (a), is to collect the reflected optical energy from the illuminated object. The planoconvex lens, which is placed at the input of the optical receiver, collects the incoming optical energy on the AQPD. To minimize the error the planoconvex aspherical lens is mostly used, because of its minimal spherical aberration coefficient. By using such a lens the most uniform distribution of the irradiance on the AQPD is achieved. The AQPD is located behind the lens at the distance d from it. Fig. 2 (b) gives the example of AQPD located in front of focal plane, e.g. $d<f$, where f is the focal length of the lens. As the AQPD isn't placed at the focal plane, a light spot with an approximately uniform distribution of irradiance is formed on its surface. The radius of the light spot is equal to r_0. From the well known geometrical relations the following equation for the spot radius is obtained:

$$r_0 = \frac{D|f-d|}{2f}, \tag{11}$$

where D is the diameter of the lens, f is the focal length and d is the distance between the lens and the AQPD.

In the case when the optical axis and the line object-receiver are not collinear, the light reflected from the object comes with a relatively small angle inclination ε_x towards the optical axis. The center of a light spot formed in such a way is moved for the distance x regarding the center of the AQPD, as it is presented on Fig. 2 (b). As the angle ε_x is small (ε_x 1), then it is easy to show that the light spot radius doesn't change significantly with the light spot movement across the AQPD. Everything above mentioned is also valid for the second plane, i.e. for the angle ε_y and for the distance y. Assuming that the reflected optical radiation is uniform, the uniform

light spot on the AQPD is obtained, as it is resented on Fig. 2 (c). Two cases are shown on this figure. The first case is when the optical axis and the line object-receiver are collinear. In that case the light spot center is at the AQPD center. In the second case the optical axis and the line object-receiver are not collinear and then the light spot is moved regarding to the AQPD center where x and y are the displacements of the light spot along the x- and y-axis, respectively.

When the centers of the light spot and the AQPD are matched all four photodiodes are illuminated with the same amount of optical radiation, so all four photodiode currents are the same. In the case when the light spot center is moved, the optical power is divided into four different parts, so the currents of each photodiode are different. By processing these currents it is possible to obtain the estimation of the distances x and y. On the basics of the determined distances it is possible to obtain the values of angle displacements ε_x and ε_y as:

$$\varepsilon_x = arctg\,\frac{x}{d} \approx \frac{x}{d}, \varepsilon_y = arctg\,\frac{y}{d} \approx \frac{y}{d}. \tag{12}$$

As it can be seen from Eq. (12), angles ε_x and ε_y are in direct proportion to the displacements of light spot center x and y, but only when the following relations are valid $|x|$ d and $|y|$ d.

One of the most important parameters of each PSOR is its field of view β, for which $\beta = 2arctg(r/d) \approx 2r/d$ is valid, where r is the AQPD radius. The maximal range of measured angles $(\varepsilon_{x,y})_{max}$, which can be measured with such an PSOR is equal to: $(\varepsilon_{x,y})_{max} = \beta/2 \approx r/d$. According to this, by the designing of geometrical parameters of the PSOR it is needed to pay the special attention should be paid to defining the minimal allowed value of the receiver field of view under which the system for positioning and tracking can function correctly. Otherwise, in certain situations the PSOR can lose the object, which can be critical especially in systems such as laser guided missiles.

A. Light Spot Displacement Measurement

Direct measurements of displacements x and y by processing signals from the AQPD isn't possible. By measuring the signals it is possible to determine the ratios of displacements and light spot radius, e.g. x/r_0 and y/r_0. For determining these relations it is essential to know the irradiance distribution on the AQPD surface. Here it is assumed for the distribution to be uniform.

The exact measurements of the ratios x/r_0 and y/r_0 aren't possible and only the estimations can be made with the following equations [3-5]:

$$\hat{x}_r = \frac{(I_I + I_{IV}) - (I_{II} + I_{III})}{(I_I + I_{IV}) + (I_{II} + I_{III})}$$

$$\hat{y}_r = \frac{(I_I + I_{II}) - (I_{III} + I_{IV})}{(I_I + I_{II}) + (I_{III} + I_{IV})}, \tag{13}$$

where $\hat{x}_r$ and $\hat{y}_r$ are the estimated values of the ratios x/r_0 and y/r_0, respectively and I_I, I_{II}, I_{III} and I_{IV}, are the AQPD peek currents. For these currents $I_K = MR_kP_K$ is valid, where M is the avalanche photodiode amplification, R_K is the photodiode conversion factor and P_K are the AQPD peek optical powers ($K=I$, II, III and IV). Finally from Eq. (13) the following is obtained for the x-axis:

$$\hat{x}_r = \frac{(P_I + P_{IV}) - (P_{II} + P_{III})}{(P_I + P_{IV}) + (P_{II} + P_{III})}. \tag{14}$$

If the irradiance on the AQPD surface is uniform then for the AQPD powers the following can be stated: $P_K = E_0 S_K$, where E_0 is the irradiance at the AQPD surface and S_K is the area of the illuminated part of the K-th quadrant of the AQPD. Taking that into consideration, we can write [5]:

$$\hat{x}_r = \frac{(S_I + S_{IV}) - (S_{II} + S_{III})}{(S_I + S_{IV}) + (S_{II} + S_{III})}. \tag{15}$$

This is the most common case in pulsed laser tracking systems.

Now it is important to find the range of the displacements x and y for which the whole light spot is located at the AQPD. This will provide a good linear dependence of x and y and the measured values at the output of the AQPD. The whole light spot is on the AQPD if the following relation is fulfilled: $\sqrt{x^2 + y^2} + r_0 \leq r$. This inequality yields to $|x| \leq r - r_0$ and $|y| \leq r - r_0$. For the angle range on the basis of Eq. (12) the following is valid: $|\varepsilon_x| \leq (r - r_0)/d$ and $|\varepsilon_y| \leq (r - r_0)/d$. According to the angle range requirements, the parameters of the AQPD such as the light spot radius r_0 and the distance between AQPD and the lens d should be determined. Wishing to provide a good linearity all four photodiodes must be illuminated. This is fulfilled if $|x| \leq r_0$ and $|y| \leq r_0$. On the basis of these inequalities, the optimal value of the light spot radius is obtained when both of these two inequalities are fulfilled at the same time, and this is when the following is satisfied: $r_0 = r - r_0$. This yields to optimal light spot radius to be $r_0 = r/2$.

To find the relations between the light spot displacements and the measured values it is necessary to determine the illuminated areas of the AQPD S_K where $K=I$, II, III and IV. For these areas, from Fig. 3, it can be written:

$$S_I + S_{IV} = r_0^2 \pi - (S_{II} + S_{III})$$
$$S_{II} + S_{III} = r_0^2 \pi \frac{\alpha}{2\pi} - \frac{1}{2} Lx \tag{16}$$

where α and L are the geometrical values which are shown on Fig. 3. For angle α the following is valid: $\alpha = 2\,arccos(x/r_0)$ and for length L: $L = 2r_0\,sin(\alpha/2)$. By substituting the last two equation in Eq. (16) the following equations is obtained:

$$S_{II} + S_{III} = r_0^2 \left[arccos\left(\frac{x}{r_0}\right) - \frac{x}{r_0}\sqrt{1 - \left(\frac{x}{r_0}\right)^2} \right], \tag{17}$$
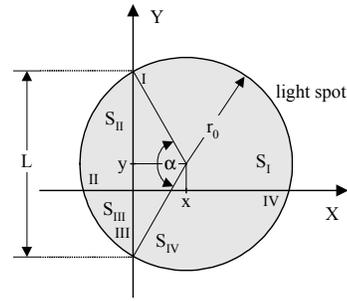

Fig. 3. Geometry of the light spot on the AQPD.

Combining Eqs. (15) to (17) finally we have for $\hat{x}_r$ the following:

$$\hat{x}_r = 1 - \frac{2}{\pi}\left[arccos\left(\frac{x}{r_0}\right) - \frac{x}{r_0}\sqrt{1 - \left(\frac{x}{r_0}\right)^2} \right]. \tag{18}$$

If we assume that the displacements are small values in regard to the light spot radius, i.e. $x \ll r_0$, we have:

$$\hat{x}_r \approx \frac{4}{\pi}\frac{x}{r_0} = S_{QPD}x, \tag{19}$$

where S_{QPD} is the AQPD incremental sensitivity. In the case of the irradiance uniform distribution: $S_{QPD} = 4/\pi r_0$.

On the basis of Eq. (19) we can obtain the estimated value of the light spot displacement $\hat{x}$, for which we can write:

$$\hat{x} = \frac{\pi}{4} r_0 \hat{x}_r = K_{QPD}\hat{x}_r, \tag{20}$$

where $K_{QPD} = 1/S_{QPD} = \pi r_0/4$ is the proportional factor between the measured and the estimated values of the light spot displacements. As it can be seen from Eq. (19) the incremental sensitivity is in an inverse proportion to the light spot radius, which means that the minimal light spot radius is needed for the maximum sensitivity.

B. Noise Induced Measurement Error

Noise, which is inherent to any electronic device, is one of the most significant causes of the angle measurement error in pulsed laser tracking systems. According to Eq. (13) and taking into consideration the equivalent noise sources, we can write:

$$\hat{x}_r = \frac{(I_I + I_{nI} + I_{IV} + I_{nIV}) - (I_{II} + I_{nII} + I_{III} + I_{nIII})}{(I_I + I_{nI} + I_{IV} + I_{nIV}) + (I_{II} + I_{nII} + I_{III} + I_{nIII})}, \tag{21}$$

where I_{ni} is the equivalent noise current of i-th photodiode. If we adopt $U = I_I + I_{IV}$ and $V = I_{II} + I_{III}$ and $U_n = I_{nI} + I_{nIV}$ and $V_n = I_{nII} + I_{nIII}$, we will obtain:

$$\hat{x}_r = \frac{(U + U_n) - (V + V_n)}{(U + U_n) + (V + V_n)}. \tag{22}$$

If we rearrange the Eq. (22) and assuming that $U_n+V_n \ll U+V$ we will get:

$$\hat{x}_r \approx \frac{U-V}{U+V} + 2\frac{VU_n - UV_n}{(U+V)^2} . \tag{23}$$

The first part of Eq. (23) represents the mean value of the relative light spot displacement and the second part represents the random error in displacement measuring caused by noise. For this measurement error $\hat{x}_{rn}$ we can write:

$$\hat{x}_{rn} \approx \frac{2V}{(U+V)^2}U_n - \frac{2U}{(U+V)^2}V_n . \tag{24}$$

As the noise sources in each receiving channel are independent, for the variance $\sigma_{\hat{x}_r}^2$ of the relative displacement measurement the following is valid:

$$\sigma_{\hat{x}_r}^2 \approx \frac{4V^2}{(U+V)^4}\sigma_u^2 + \frac{4U^2}{(U+V)^4}\sigma_v^2 , \tag{25}$$

where σ_u^2 and σ_v^2 are the variances of the U_n and V_n, respectively and $\sigma_u^2 = \sigma_v^2 = 2\overline{i_n^2}$, where $\overline{i_n^2}$ is the variance of the noise current in each receiving channel. Now, Eq. (25) can be rearranged in:

$$\sigma_{\hat{x}_r}^2 \approx 8\frac{U^2+V^2}{(U+V)^4}\overline{i_n^2} . \tag{26}$$

As for U and V, $S_S=U+V$ is valid, where S_S is the signal in the summing channel, the variance $\sigma_{\hat{x}_r}^2$ of the relative displacement measurement becomes:

$$\sigma_{\hat{x}_r}^2 \approx 8\frac{U^2+(S_S-U)^2}{S_S^4}\overline{i_n^2} . \tag{27}$$

The variance $\sigma_{\hat{x}_r}^2$, from Eq. (27), has the minimum value for $U=S_S/2$ and $V=S_S/2$, so we can write:

$$\left(\sigma_{\hat{x}_r}^2\right)_{min} \approx \frac{4\overline{i_n^2}}{S_S^2} = \frac{1}{SNR_\Sigma}, \tag{28}$$

where SNR_Σ is signal-to-noise ratio in summing channel. As it can be seen, the minimal variance of the relative displacement measurement is achieved when $U=V=S_S/2$ is valid, i.e. when the light spot center is at the AQPD center. According to Eq. (20), for the minimal value of the estimated light spot displacement standard deviation $\left(\sigma_{\hat{x}}\right)_{min}$ we have:

$$\left(\sigma_{\hat{x}}\right)_{min} \approx \frac{\pi}{4}\frac{r_0}{\sqrt{SNR_\Sigma}} . \tag{29}$$

The identical expression is valid for the standard deviation $\left(\sigma_{\hat{y}}\right)_{min}$ of the estimated displacement along the y-axis. On the basics of Eqs. (12) and (29) for the minimal standard deviation $\left(\sigma_{\varepsilon_x}\right)_{min}$ of measured angle, in the case of uniform irradiance distribution, we have:

$$\left(\sigma_{\varepsilon_x}\right)_{min} \approx \frac{\pi}{4}\frac{r_0}{d}\frac{1}{\sqrt{SNR_\Sigma}} . \tag{30}$$

The parameters U and V are satisfy the following inequalities: $U \leq S_S$ and $V \leq S_S$. Because of that and according to Eq. (27), the maximal value of the $\left(\sigma_{\hat{x}}\right)_{max}$ is achieved when $U=S_S$ and $V=0$ (or $V=S_S$ and $U=0$) is fulfilled, i.e. when the light spot center is at the measurement span margin ($x=\pm r_0$ and/or $y=\pm r_0$), so we have:

$$\left(\sigma_{\hat{x}}^2\right)_{max} \approx \frac{2}{SNR_\Sigma} . \tag{31}$$

Identically, for the maximal standard deviation of estimated displacement along the x-axis $\left(\sigma_{\hat{x}}\right)_{max}$ and the measured angle $\left(\sigma_{\varepsilon_x}\right)_{max}$, are valid:

$$\left(\sigma_{\hat{x}}\right)_{max} \approx \frac{\pi\sqrt{2}}{4}\frac{r_0}{\sqrt{SNR_\Sigma}} \text{ and} \tag{32}$$

$$\left(\sigma_{\varepsilon_x}\right)_{max} \approx \frac{\pi\sqrt{2}}{4}\frac{r_0}{d}\frac{1}{\sqrt{SNR_\Sigma}} . \tag{33}$$

The identical expressions are valid for the maximal standard deviation of estimated displacement along the y-axis $\left(\sigma_{\hat{y}}\right)_{max}$ and the measured angle $\left(\sigma_{\varepsilon_y}\right)_{max}$. As it can be seen, the maximal standard deviation of measured displacements and angles are $\sqrt{2}$ times bigger than their minimal values, which doesn't represent a significant enlargement. For us of interest is the minimal error in positioning and tracking, because in the case when the centers of the light spot and the AQPD are matched, we have a good positioning and tracking.

The required span of the measured angles depends on the dynamics of the pulsed laser tracking system. This measurement span is determined by the receiving optics field-of-view β. The receiving optics is designed in such a way to cover, with its field-of-view, the complete range of measured angles. According to Eq. (30) and the relations between the field-of-view, the AQPD radius and the light spot radius, for the noise induced angle measurement error $\sigma_{\varepsilon n}$ we can write:

$$\sigma_{\varepsilon n} \approx \frac{\pi}{16}\beta\frac{1}{\sqrt{SNR_\Sigma}} . \tag{34}$$

As it can be seen from Eq. (34), it is recommended to choose the value of field of view as minimal as possible to minimize the angle measurement error. On the basis of Eq. (11) and the relations between field-of-view and the remaining OEC parameters and if $\beta \ll 1$ is satisfied, there is a relation between the AQPD radius and the receiving optics aperture diameter: $r \approx \beta f_{no}D/2$, where f_{no} is the f-number of the lens, for which $f_{no} = f/D$ is valid.

IV. TRANSIMPEDACE AMPLIFIER

As the first stage, in the analog signal processing from the AQPD, the transimpedance amplifiers (TIA) have two main functions. The first is to filter the noises at their inputs and the second function is to amplify the current signals from the AQPD. The current signals at the AQPD are converted into voltage signals, at these amplifiers, to be more suitable for further analog signal processing. The optimization of these amplifiers is essential, because it can be the main limiting factor of the whole receiving channel. The electrical scheme of the TIA and the AQPD is shown on Fig. 4 with all the relevant elements.
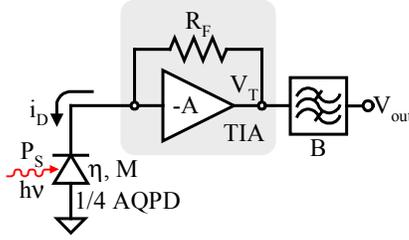

Fig. 4. The AQPD and the TIA.

The voltage signal at the TIA output V_T is equal to $V_T=R_F i_D$, where R_F is the resistance of the feedback resistor. Further, this signal is processed by the bandpass filter with the bandwidth equal to B. The function of this filter is to limit the noise level at the TIA output. The bandwidth B must provide on the one hand, the undisturbed passing through of the useful signal and on the other hand, the maximal noise filtering. These two conflict requirements can be resolved by choosing the minimal value for bandwidth B, which can provide complete reconstruction of an input signal. This minimal value is equal to $B \approx 0.35/t_r$, where t_r is the rise time of an input signal, which is defined as $t_r = t_{90\%} - t_{10\%}$, where $t_{90\%}$ and $t_{10\%}$ are the times when the signal is at its 90% and 10% from its maximal value, respectively. In the case when we have a Gaussian pulse, which is satisfied when the Q-switched Nd:YAG laser is used as a designator, with full width at half maximum (FWHM) equal to τ we have: $t_r = 0.716\tau$ and $B \approx 0.49/\tau$.

To determine the angle measurement error, first we must calculate the signal-to-noise ratio SNR_Σ in the summation channel. For that reason, it is necessary to determine the equivalent input noise current in each channel. Fig. 5 gives the optimal structure of the TIA [10] with all the relevant parameters for determining the equivalent input noise current in one channel.
The signal-to-noise ratio SNR_Σ in the summation channel is equal to:

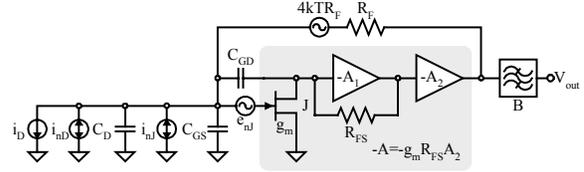$$SNR_\Sigma = \frac{I_S^2}{4\overline{i_n^2}}, \qquad (35)$$

Fig. 5. The optimal structure of the TIA.

where $I_s = R_k M P_s$ and the equivalent noise current $\overline{i_n^2}$ [11]:

$$\overline{i_n^2} = B\left[\overline{i_{nD}^2} + \overline{i_{nJ}^2} + \frac{4kT}{R_F} + \frac{4\pi^2}{3}\overline{e_{nJ}^2}(C_D + C_G)^2 B^2\right], \qquad (36)$$

where $\overline{i_{nD}^2}$ is the avalanche photodiode noise current for which we have:

$$\overline{i_{nD}^2} = 2q\left[I_{DR}^S + \left(I_{DR}^V + I_{BG} + \frac{I_S}{4}\right)M^2 F(M)\right], \qquad (37)$$

where q is the electronic charge, I_{DR}^S is the dark surface current, I_{DR}^V is the dark bulk current, $I_{BG} = R_k P_{BG}/4$ is the background current and $F(M) = M^n$ is the avalanche photodiode excess noise factor.

The equivalent noise current of the input transistor J $\overline{i_{nJ}^2}$ can be neglected, because a GaAs MESFET is used as the first stage in TIA. For equivalent input voltage noise $\overline{e_{nJ}^2}$ of a MESFET we have:

$$\overline{e_{nJ}^2} = \frac{4\Gamma kT}{g_m}, \qquad (38)$$

where for GaAs MESFET $\Gamma=1.5$ is valid, k is Boltzmann's constant, T is the absolute temperature and g_m is the transconductanse of an input transistor. In Eq. (38) we have omitted the flicker noise because it is dominant only on relatively low frequencies.

The remaining parameters from Eq. (36): C_D is the AQPD segment capacitance and $C_G = C_{GS} + C_{GD}$ is the input capacitance of the TIA, where C_{GS} and C_{GD} are the capacitances between gate and source and between gate and drain of the MESFET, respectively.

On the basis of the above analysis it can be noticed that there is the optimal value of avalanche photodiode amplification M_{opt}, for which the maximal signal-to-noise ratio in the summation channel is gained. This optimal value is equal to:

$$M_{opt} = \left[\frac{2qI_{DR}^S + \frac{4kT}{R_F} + \frac{4\pi^2}{3}\overline{e_{nJ}^2}(C_D + C_G)^2 B^2}{nq\left(I_{DR}^V + I_{BG} + \frac{I_S}{4}\right)}\right]^{\frac{1}{2+n}}. \qquad (39)$$

On the other side, the tranconductance of the MESFET g_m and the input capacitance C_G are connected with $g_m = K_J C_G$, where constant K_J depends on MESFET channel length. For a

MESFET with 1μm channel length $K_J\approx90mS/pF$ is valid. It is possible to select the optimal MESFET channel width, which provides the minimal value of equivalent voltage noise at the preamplifier input. The channel width is selected to fulfill the relation $C_D=C_G$.

The AQPD parameters such as the segment capacitance, the dark surface current and the dark bulk current depend on the AQPD radius in such a way that the segment capacitance and the dark bulk current depend on the segment area and the dark surface current depends on the segment arc length along the AQPD circumference [1] and [12]. Relations between these parameters are: $C_D = K_C\,\pi r^2/4$, $I_{DR}^S = K_S\,\pi r/2$ and $I_{DR}^V = K_V\,\pi r^2/4$, where K_C, K_S and K_V are the corresponding constants that depend on the used technology. In order to minimize the overall noise it is important to select the technology which will keep those constants as minimal as possible. It is also important that the AQPD radius be as minimal as possible, but there are some limitations such as the minimal value of the receiving optics field-of-view. In that case, it is necessary to select the lens which has a minimal value of f-number.

V. ATMOSPHERE INDUCED ERRORS

Atmospheric turbulence causes phenomena commonly referred to as beam wander, scintillation and beam breathing, according to the effect produced on the beam spot as seen on the screen after traveling through a turbulent atmosphere. Beam wander means random changes in the position of the beam spot on the screen, in the scintillation illumination fluctuations within the beam and also in the breathing expansion and contraction of the spot beyond the dimensions predicted by its geometry and diffraction. These effects are caused by index-of-refraction inhomogeneities which mainly arise from spatial temperature differences within the atmosphere.

A turbulent atmosphere can be thought to be composed of cells of various sizes that differ in their index of refraction. As these cells move across a beam of light, they cause the effects described above. According to this "frozen" atmosphere assumption, the velocity and direction of this uniform motion is determined by the mean wind speed.

Depending on the dominant cell size and beam diameter, turbulent cells affect light propagation in different ways. Cells that are larger than the beam diameter act like weak lenses and deflect the beam as a whole in a random way (angle of wave front) leaving its irradiance distribution essentially unaltered (beam wander), but when the cell size is smaller than the diameter of the beam, refraction and diffraction take place and the irradiance profile of the beam breaks up into small bright and dark areas as a result of refracted and diffracted wave front interference (scintillation). Depending on the relative strength of the turbulence either of the effects may be observed, or both simultaneously. The dominant effect is beam wander in weak turbulence and scintillation in strong turbulence [13].

The strength of atmospheric turbulence is described by the refractive index structure coefficient C_n, which is basically a measure of the spatial gradient of the refractive index (temperature) within the atmosphere. From the sensor point of view the strength of the turbulence also depends on the length of the path that the light traverses. The strength of path-integrated turbulence is described by the spherical wave coherence length $\rho_0 = \left(0.545\kappa^2 RC_n^2\right)^{-3/5}$ [6], where $\kappa = 2\pi/\lambda$ and R is the distance that the beam travels in a turbulent atmosphere. This describes the amount of scattering caused by atmospheric turbulence and is used to determine whether the turbulence in a particular case is considered weak or strong. Turbulence is considered to be weak if ρ_0 is larger than the diffraction patch size $\sqrt{R\lambda}$ and strong if it is smaller [14]. The following classification of the turbulence strength can also be found: $C_n=8\times10^{-9}\text{m}^{-1/3}$ weak turbulence, $C_n=4\times10^{-8}\text{m}^{-1/3}$ middle turbulence and $C_n=5\times10^{-7}\text{m}^{-1/3}$ strong turbulence [15].

The effect of atmospheric turbulence on beam propagation is a result of complicated phenomena. In certain cases, however, it can be satisfactorily estimated using simple equations. Geometric optical formulation, for example, can be successfully used to predict large-scale effects such as angle-of-arrival fluctuations or beam wander [14] and [16-20]. This presupposes, however, that the beam diameter ϕ should not be markedly altered by diffraction, or by scattering due to atmospheric turbulence. The first condition is fulfilled if the measurement distance is within the Fresnel diffraction range ($\phi > \sqrt{R\lambda}$) and the second condition if the path-integrated turbulence is weak ($\rho_0 > \sqrt{R\lambda}$) [14].

The various mechanisms by which the measurement precision of a reflected beam sensor is affected include angular fluctuations in the wave front, irradiance fluctuations at a misfocused receiver aperture and irradiance fluctuations. Simple equations are presented below for estimating the magnitude of the above effects. The derivations were performed by combining the results of several publications.

A. Angle-of-Arrival Fluctuations

The angle of arrival is the average tilt of a wave front across the receiver aperture, and is thus the same as the angle (direction) of the received beam. A general form for the equation required estimating the variance in angle-of-arrival fluctuations $\sigma_{\varepsilon a}^2$ is [6]:

$$\sigma_{\varepsilon a}^2 = \varphi C_n^2 D^{-\frac{1}{3}} R, \qquad (40)$$

where φ is a constant, D is the aperture diameter and R is the distance that the beam travels in a turbulent atmosphere before reaching the aperture. On the basis of [6] the constant φ is equal to $\varphi\approx0.79$. As the reflected beam travels the path from the object to the receiving optics, we have $R=R_M$, so for the variance in angle-of-arrival fluctuations we have:

$$\sigma_{\varepsilon a}^2 = \varphi C_n^2 D^{-\frac{1}{3}} R_M. \qquad (41)$$

B. Effect of Irradiance Fluctuations

Irradiance fluctuations caused by atmospheric turbulence affect precision if the receiver is misfocused. Atmospheric turbulence causes the received irradiance to fluctuate across the receiver aperture. These fluctuations cause no problems in a focused case, because each elemental area of the receiver images the light collected by it onto the entire image spot. In this situation the irradiance fluctuations related to the elemental area change the irradiance of the image spot uniformly leaving its centroid unaltered. In a misfocused receiver, however, the irradiance fluctuations across the receiver aperture are directly projected on the light spot on the AQPD surface. These spatially uncorrelated fluctuations then cause variation in the light spot centroid and affect measurement precision. In the case of a misfocused AQPD receiver the standard deviation $\sigma_{\varepsilon i}$ of the measured object position due to irradiance fluctuations is [6]:

$$\sigma_{\varepsilon i} \approx \frac{\pi}{8} \frac{r_0}{d} \sqrt{\frac{1-c_c}{SFR}} = \frac{\pi}{32} \beta \sqrt{\frac{1-c_c}{SFR}} , \qquad (42)$$

where c_c is the correlation coefficient of the irradiance fluctuations between crosswise quadrants of the circular receiver aperture and *SFR* is the signal-to-fluctuation ratio related to one quadrant of the receiver aperture defined as the average signal power divided by the rms value of its fluctuations [21].

In the case of narrow band laser irradiance the spatial correlation depends on the effective distance of the crosswise receiver aperture quadrants in relation to the Fresnel zone size $\sqrt{R\lambda}$, and the *SFR* on the path-integrated turbulence strength and the averaging provided by the receiver aperture quadrant [22]. It can be concluded from [23-26] that if the receiver is illuminated directly by a point source and two receiver points have a lateral separation larger than about $D_K \approx 0.6\sqrt{R_M \lambda}$, c_c is essentially zero. This means that the irradiance fluctuations of crosswise receiver quadrants should be uncorrelated when practical aperture sizes of a few cm and measurement distances up to a couple of hundred meters are used. In the case of pulsed laser tracking systems for $R_M \approx 10$km and $\lambda = 1.064\mu$m, the minimal lateral separation between two receiver points, for which we have correlation coefficient approximately equal to zero, is approximately 6cm. As the receiver aperture could be several cm in diameter, we can assume that $c_c \neq 0$ and as it is valid for $D=0$ the correlation coefficient is $c_c \approx 1$ and for $D \geq D_K$ the correlation coefficient is $c_c \approx 0$, we can make the assumption that the correlation coefficient c dependence on the aperture diameter D is linear, so:

$$c_c = \begin{cases} 1 - \dfrac{D}{D_K}, & D \leq D_K \\ 0, & D > D_K \end{cases} , \qquad (43)$$

where $D_K = 0.6\sqrt{R_M \lambda}$.

In the case of narrow band irradiance, the *SFR* can be deduced in the following way. In weak turbulence the normalized irradiance variance for a point receiver illuminated by a diverging beam is $\sigma_{Ipr}^2 = 0.496\kappa^{7/6} R_M^{11/6} C_n^2$ [27]. This magnitude of fluctuations is reduced by aperture averaging, so for the normalized irradiance variance σ_{Ier}^2 we have:

$$\sigma_{Ier}^2 = \frac{\sigma_{Ipr}^2}{A_\gamma} , \qquad (44)$$

where A_γ is:

$$A_\gamma = 1 + 0.362\gamma^{-\frac{7}{3}} , \qquad (45)$$

and $\gamma = D / \sqrt{R_M \lambda}$ [27]. Finally for *SFR* we have $SFR = 1 / \sigma_{Ier}^2$. By combining Eq. (42), (44) and (45) we finally obtain for *SFR*:

$$SFR = \frac{1 + 0.362\left(\dfrac{D}{\sqrt{R_M \lambda}}\right)^{-\frac{7}{3}}}{0.496\kappa^{\frac{7}{6}} R_M^{\frac{11}{6}} C_n^2} . \qquad (46)$$

On the basis of Eq. (42) and (46), for the standard deviation $\sigma_{\varepsilon i}$ of measured angles caused by the irradiance fluctuation on the AQPD surface we have:

$$\sigma_{\varepsilon i} = \frac{\pi}{32} \beta \sqrt{1-c_c} \left[\frac{0.496\kappa^{\frac{7}{6}} R_M^{\frac{11}{6}} C_n^2}{1 + 0.362\left(\dfrac{D}{\sqrt{R_M \lambda}}\right)^{-\frac{7}{3}}} \right]^{\frac{1}{2}} . \qquad (47)$$

VI. TOTAL ANGLE MEASUREMENT ERROR

There are three main factors which cause the angle measurement error: random noise in the receiver channel, angle-of-arrival fluctuations and irradiance fluctuations on the AQPD surface. All these measurement errors are characterized by their variances. As these random processes are independent, for the variance $\sigma_{\varepsilon TOT}^2$ of the total angle measurement error we have:

$$\sigma_{\varepsilon TOT}^2 = \sigma_{\varepsilon n}^2 + \sigma_{\varepsilon a}^2 + \sigma_{\varepsilon i}^2 . \qquad (47)$$

In any control system for automatic positioning and tracking there is the maximal allowed error in angle measurement for which the system is functional. The value of this maximal allowed error depends on the actual system realization. The common accepted value for the maximal allowed standard deviation of this error is 2mrad. On the basis of this accepted value, the maximal operating range for positioning and tracking can be defined. In that case for the maximal range R_D, defined in the way as it is described above the following is valid: $R_D = R_M(\sigma_{\varepsilon TOT} = 2mrad)$, where

$R_M\left(\sigma_{\varepsilon TOT} = 2mrad\right)$ is the distance between the illuminated object and the receiver at which the total angle measurement error is equal 2mrad. On Fig. 6 the dependence between the maximal range R_D and the receiver aperture diameter D for the following parameters is presented: laser peak power P_L=5MW, FWHM of the laser pulse τ=20ns (energy per laser pulse is approximately equal to $E_L\approx$100mJ), field-of-view of the receiving optics β=10°, MESFET constant K_J=90mS/pF, MESFET excess noise factor Γ=1.5, optical filter spectral bandwidth Δ_λ=1nm, receiving optics transmission coefficient T_R=0.9, optical filter transmission coefficient T_F=0.4, refractive index structure coefficient C_n=8×10^{-9}m$^{-1/3}$ (this value for the refractive index structure coefficient is taken because it represents the mean value in the case of weak turbulence), avalanche photodiode excess noise factor coefficient n=0.4, transimpedance resistance R_F=10kΩ, avalanche photodiode conversion coefficient for unit gain R_k=0.45A/W, avalanche photodiode technology coefficients K_C=1pF/mm^2, K_S=3×10^{-8}A/mm, K_I=1×10^{-10}A/mm^2 [28], f-number of the aspheric planoconvex lens f_{no}=0.7, background reflectance ρ_B=0.4, target reflectance ρ_T=0.2, atmospheric extinction coefficient σ=0.15 1/km, laser-object distance R_L=2km, angle between object surface normal and the line joining the object and receiver centers θ=45°, transmission coefficient of transmitting optics T_T=0.9, transmitting optics collection efficiency η=0.6, absolute temperature T=300K and for solar spectral irradiance three values were taken E_λ=50, 300 and 600W/(m^{2}μm).
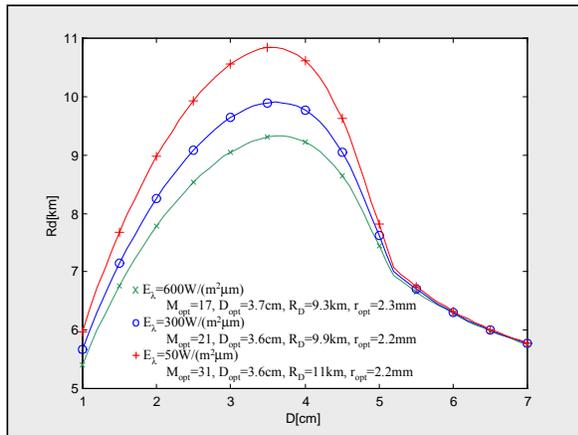

Fig. 6. The maximal range dependence on the aperture diameter.

As it can be seen from Fig. 6 there is an optimal value of the receiving optics aperture diameter D_{opt} for which the pulsed laser tracking system has the maximal positioning and tracking range. Although we have changed the value of solar spectral irradiance in the wide range, the optimal value of the receiving optics aperture diameter has just slightly changed. The optimal value of this diameter is in the range of 3.6cm to 3.7cm. The optimal avalanche photodiode amplification is also changed in the relatively narrow range from 17 to 31. Concerning the optimal aperture diameter and the minimal allowed field-of-view, the optimal radius of he AQPD has, also, just slightly changed.

VII. Conclusion

Concerning the maximal range of positioning and tracking in pulsed laser tracking systems the optimal parameters of an optical receiver was found. It was shown that there is an optimal receiving optics aperture diameter which is slightly changed by changing the solar irradiance conditions. The optimal diameter is approximately equal to 3.6cm for a standard set of parameters, as shown in Part 0. This optimal diameter value is in good matching with the aerodynamical requirements for laser guided missiles. Also, the optimal value of the AQPD radius was found to be equal to approximately 2.2mm. This yields to the maximal possible range to be equal approximately 10km.

References

[1] H. N. Burns, C. G. Christodoulou, G. D. Boerman, „System Design of a Pulsed Laser Rangefinders", *Optical Engineering*, Vol. 30, No. 3, pp 323-329, March 1991.

[2] Zarko Barbaric and Mirjana Nikolic, „Parametrical Analysis of Pulsed Laser Rangefinder's Range", *XLII ETRAN Conference Proceedings*, Vrnjacka Banja, 3-5 Jun 1998.

[3] W. L. Wolfe and G. J. Zissis, „The Infrared Handbook", Ann Arbor, Environmental Research Institute of Michigan, 1978.

[4] Ernest O. Doebelin, *Measurement Systems Application and Design*, Mc Graw-Hill, 1990.

[5] Leonid G. Kazovsky, „Theory of Tracking Accuracy of Laser Systems", *Optical Engineering*, Vol. 22, No. 3, pp 339-347, May/June 1983.

[6] Anssi Mäkynen, *Position-Sensitive Devices and Sensor Systems for Optical Tracking and Displacement Sensing Applications*, Academic Dissertation, University of Oulu, Department of Electrical Engineering, Oulu, 2000.

[7] A. Mäkynen, J. Kostamovaara and R. Myllylä, „Positioning Resolution of the Position-Sensitive Detectors in High Background Illumination", *IEEE Transactions on Instrumentation and Measurement*, Vol. 45, No. 1, pp 324-326, 1996.

[8] Y. Yanhai, „The Design of Echo Spot and Optical Focusing in Automatic Laser Tracking", *Optics and Laser Technology*, Vol. 18, No. 2, pp 75-79, 1986.

[9] P. W. Young, L. M. German and R. Nelson, „Pointing, Acquisition and Tracking Subsystems for Space-Based Laser Communications", *Proceedings of SPIE 616*, pp 118-128, 1986.

[10] J. L. Hullett and S. Moustakas, „Optimum Transimpedance Broadband Optical Preamplifier Design", *Optical and Quantum Electronics*, 13, pp 65-69, 1981.

[11] Lazo M. Manojlovic, *Analysis and Optimization in Receiving Optical Signal from Optoelectronic Coordinator in Pulsed Laser Tracking Systems*, Master Thesis, Electrotechnical Faculty, University of Belgrade, Belgrade, 2003.

[12] Hiroaki Ando, Hiroshi Kanbe, Tatsuya Kimura, Toyoshi Yamaoka and Takao Kaneda, „Characteristics of Germanium Avalanche Photodiodes in the Wavelength Region of 1-1.6μm", *IEEE Journal of Quantum Electronics*, Vol. QE-14, No. 11, pp 804-809, 1978.

[13] H. Weichel, „Laser Beam Propagation in the Atmosphere", *SPIE*, Bellingham, Washington, USA, pp 45-66, 1990.

[14] J. H. Churnside and R. J. Lataitis, *Statistics of a Reflected Beam in the Turbulent Atmosphere (Path Correlation)*, NOAA Technical Memorandum ERL WPL-172, National Oceanic and Atmospheric Administration, Environmental Research Laboratories, Wave Propagation Laboratory, Boulder, Colorado, USA, 1989.

[15] Ж. Госсорг, *Инфракрасная термография – Основы, механика, применение*, Мир, Москва, 1988.

[16] R. S. Lawrence and J. W. Strohbehn, „A Survey of Clear-Air Propagation Effects Relevant to Optical Communications", *Proceedings of the IEEE*, Vol. 58, No. 10, pp 1523-1545, 1970.

[17] T. Chiba, „Spot Dancing of the Laser Beam Propagated Through the Turbulent Atmosphere", *Applied Optics*, Vol. 10, No. 11, pp 2456-2461, 1971.

[18] J. W. Dowling and P. M. Livingston, „Behavior of Focused Beams in Atmospheric Turbulence: Measurements and Comments on the Theory", *Journal of the Optical Society of America*, Vol. 63, No. 7, pp 846-858, 1973.

[19] J. H. Churnside and R. J. Lataitis, „Angle-of-Arrival Fluctuations of a Reflected Beam in Atmospheric Turbulence", *Journal of Optical Society of America A*, Vol. 4, No. 7, pp 1264-1272, 1987.

[20] J. H. Churnside and R. J. Lataitis, „Wander of an Optical Beam in the Turbulent Atmosphere", *Applied Optics*, Vol. 29, No. 7, pp 926-930, 1990.

[21] G. A. Andreev and R. M. Magind, *Influence of Intensity Fluctuations on the Measurement of Angular Position of Radiation Source by Optical-Electron Monopulse Method*, Izvestiya Vysshikh Uchebnykh Zavedenii Radiofizika, Vol. 15, No. 1, pp 55-61, 1972.

[22] A. Mäkynen, J. Kostamovaara and R. Myllylä, „Displacement Sensing Resolution of Position-Sensitive Detectors in Atmospheric Turbulence Using Retroreflected Beam", *IEEE Transactions on Instrumentation and Measurement*, Vol. 46, No. 5, pp 1133-1136, 1997.

[23] R. S. Lawrence and J. W. Strohbehn, „A Survey of Clear-Air Propagation Effects Relevant to Optical Communications", *Proceedings of the IEEE*, Vol. 58, No. 10, pp 1523-1545, 1970.

[24] R. L. Fante, „Electromagnetic Beam Propagation in Turbulent Media", *Proceedings of the IEEE*, Vol. 63, No. 12, pp 1669-1692, 1975.

[25] W. A. Coles and R. G. Frechlich, „Simultaneous Measurement of Angular Scattering and Intensity Scintillation in the Atmosphere", *Journal of Optical Society of America*, Vol. 72, No. 8, pp 1042-1048, 1982.

[26] J. H. Churnside and J. J. Wilson, „Enhanced Backscatter of a Reflected Beam in Atmospheric Turbulence", *Applied Optics*, Vol. 32, No. 15, pp 2651-2655, 1993.

[27] H. Weichel, „Laser Beam Propagation in the Atmosphere", *SPIE*, Bellingham, Washington, USA: 45-66, 1990.

[28] P. E. Webb, R. J. McIntyre, and J. Conardi, *Properties of Avalanche Photodiodes*, Technical Report, RCA, 1977.